Mon. Not. R. Astron. Soc. **363,** 1083–1091 (2005) doi:10.1111/j.1365-2966.2005.09542.x

Collisional excitation rate coefficients of N_2H^+ by He

F. Daniel,[1⋆] M.-L. Dubernet,[1⋆] M. Meuwly,[2] J. Cernicharo[3] and L. Pagani[1]

[1] *Observatoire de Paris-Meudon, LERMA UMR CNRS 8112, 5, Place Jules Janssen, F-92195 Meudon Cedex, France*
[2] *Department of Chemistry, University of Basel, Klingelbergstrasse 80, 4056 Basel, Switzerland*
[3] *DAMIR-IEM-CSIC, C/Serrano, 113-121, 28006 Madrid, Spain*

Accepted 2005 August 18. Received 2005 August 18; in original form 2005 April 11

ABSTRACT

Using a recoupling technique with close-coupling spin-free calculations de-excitation rate coefficients are obtained among hyperfine transitions for He colliding with N_2H^+. A recently determined potential energy surface suitable for scattering calculations is used to investigate rate coefficients for temperatures between 5 and 50 K, and for the seven lowest rotational levels of N_2H^+. Fitting functions are provided for the Maxwellian averaged opacity tensors and for the rotational de-excitation collisional rate coefficients. The fitting functions for the opacity tensors can be used to calculate hyperfine (de)-excitation rate coefficients among elastic and inelastic rotational levels, and among the corresponding magnetic sublevels of the hyperfine structure. Certain dynamical approximations are investigated and found to be invalid.

Key words: molecular data – molecular processes – methods: numerical – ISM: molecules.

1 INTRODUCTION

Together with HCO^+, N_2H^+ was one of the first molecular ions detected in interstellar space (Thaddeus & Turner 1975). The $J = 1 - 0$ line of this species has been extensively observed towards cold dark clouds and protostellar cores in order to characterize the physical conditions of the gas (Bergin et al. 2002; Tafalla et al. 2004; Hotzel, Harju & Walmsley 2004; Belloche et al. 2002; Caselli et al. 2002). These observations indicate that N_2H^+ traces the highest density regions of dark clouds. Unlike CO and other molecular species, it seems that N_2H^+ is less depleted on to dust grain surfaces, which is probably related to the fact that N_2, the chemical precursor of N_2H^+, is more volatile than CO and condensates at lower temperatures than carbon monoxide. In addition, the complex hyperfine structure of N_2H^+ always allows at least one of the hyperfine line components to be optically thin. This allows the study of the innermost regions of cold dark clouds contrary to the large opacities that affect other molecular ions such as HCO^+ (Cernicharo & Guelin 1987).

The presence of many components in the line profile of the $J = 1 - 0$ line (and also in higher-J rotational lines) should permit one to model the physical conditions and the physical structure of the clouds better than from single line profile observations (HCO^+ or CS for example). However, only very crude estimates have been obtained so far for these parameters due to the lack of collisional rates between N_2H^+ and molecular hydrogen (or helium). The observational data indicate some hyperfine intensity anomalies that could be due to selective collisional processes or to radiative transfer effects [see Gonzalez-Alfonso & Cernicharo (1993), for the interpretation of the hyperfine intensities of HCN in dark clouds]. It is clear that in order to interpret and to model the observations of N_2H^+, the state-to-state collisional rates of this molecule with H_2 and He are required by the experimentalists. This information will be even more necessary when ALMA (Atacama Large Millimeter Array) will provide high angular resolution and high-sensitivity observations of protostellar cores in several rotational lines of N_2H^+. N_2H^+ has been also detected in warm molecular clouds where the lines are broader and very strong. In these objects only the hyperfine structure due to the outer N atom could be observed as the splitting produced by the inner N atom is lower than the intrinsic line width. Nevertheless, to correctly model the emerging intensity from N_2H^+ in these clouds, astronomers require a complete set of state-to-state collisional rates. From an astrophysical point of view, collisional rates for N_2H^+ for kinetic temperatures applying to cold dark clouds and warm molecular clouds, 5–50 K, are needed.

In a previous paper (Daniel, Dubernet & Meuwly 2004) a new potential energy surface for the He–N_2H^+ system has been reported and the formalism to calculate collisional excitation cross-sections between N_2H^+ hyperfine levels and propensity rules among hyperfine cross-sections has been discussed in detail. The cross-sections between hyperfine levels were obtained using a recoupling technique for the case of two nuclear spins and were expressed in terms of opacity tensors calculated with a close-coupling (CC) method. In the present paper we provide the fits to the collisional de-excitation rate coefficients for rotational transitions among the lowest seven rotational levels of N_2H^+ in collision with He, and the fits to the Maxwellian average of the opacity tensors. The latter can be used to obtain the de-excitation rate coefficients among hyperfine levels and among magnetic sublevels of the hyperfine structure in the

⋆E-mail: fabien.daniel@obspm.fr (FD); marie-lise.dubernet@obspm.fr (MLD)

temperature range from 5 to 50 K, for both inelastic and elastic rotational transitions. These data are of central interest to the astronomy community.

This work is structured as follows. Section 2 discusses the hyperfine energy levels of N_2H^+, the methodology used to obtain the rate coefficients and their analytical representation. Section 3 presents comparisons between our rotational de-excitation rate coefficients and those calculated previously, and addresses the issue of the validity of simpler approaches.

2 METHODOLOGY

The energy levels of N_2H^+ are characterized with the quantum numbers j, F_1 and F, where j is the rotational quantum number, F_1 results from the coupling of $\hat{j}$ with $\hat{I}_1(\hat{F}_1 = \hat{j} + \hat{I}_1)$ where $I_1 = 1$ is the nuclear spin of the outer nitrogen, and $\hat{F} = \hat{F}_1 + \hat{I}_2$ with $I_2 = 1$ the nuclear spin of the inner nitrogen. F is the only good quantum number, although the mixing between different j and F_1 components is very small, so that the energy levels are still well characterized by j and F_1. The external nucleus induces the largest splittings because its coupling constants are larger than those of the internal nucleus. The hyperfine energy levels can be found by diagonalizing the molecular Hamiltonian $H_{\rm mol} = B\hat{j}^2 - D\hat{j}^4 + H_{\rm coupling}$, where B and D are the rotational and centrifugal distortion constants of the molecule and $H_{\rm coupling}$ is the effective nuclear coupling Hamiltonian (Caselli, Myers & Thaddeus 1995; Gordy & Cook 1984):

$$H_{\rm coupling} = \sum_{k=1}^{2} \left\{ \frac{(eQq_{j'j})_k}{2I_k(2I_k-1)j(2j-1)} \times \left[3(\boldsymbol{I}_k\cdot\boldsymbol{j})^2 + \frac{3}{2}(\boldsymbol{I}_k\cdot\boldsymbol{j}) - \boldsymbol{I}_k^2\cdot\boldsymbol{j}^2 \right] + (C_j)_k(\boldsymbol{I}_k\cdot\boldsymbol{j}) \right\} \quad (1)$$

The $eQq_{j'j}$ and C_j coefficients are coupling coefficients which depend on the moments of inertia of the molecule. They are related to the electrostatic quadrupolar and magnetic dipolar coupling constants. Energy levels shown in Table 1 are obtained with new rotational and coupling constants based on the observations of Caselli et al. (1995) and provided by P. Caselli & L. Dore (private communication). For each rotational level ($j > 1$) there are nine hyperfine levels. Table 1 gives the hyperfine energy levels with their quantum labelling.

Hyperfine de-excitation rate coefficients can be obtained from a Maxwellian average either of the hyperfine de-excitation cross-sections or from equation (15) of Daniel et al. (2004), namely:

$$R_{jF_1F\to j'F_1'F'}(T) = \frac{1}{[F]}\sum_K \left\langle \frac{\pi}{k^2} P^K_{jF_1F,j'F_1'F'} \right\rangle_T \quad (2)$$

with $[F] = 2F + 1$,

$$\left\langle \frac{\pi}{k^2} P^K_{jF_1F,j'F_1'F'} \right\rangle_T = [F_1F_1'FF'] \begin{Bmatrix} j & j' & K \\ F_1' & F_1 & I_1 \end{Bmatrix}^2 \times \begin{Bmatrix} F_1 & F_1' & K \\ F' & F & I_2 \end{Bmatrix}^2 \left\langle \frac{\pi}{k^2} P^K_{jj'} \right\rangle_T \quad (3)$$

and

$$\left\langle \frac{\pi}{k^2} P^K_{jj'} \right\rangle_T = \sqrt{\frac{8}{\mu\pi}}(k_BT)^{-3/2}\frac{\hbar^2}{2\mu} \times \int_0^\infty P^K_{jj'}(E)\mathrm{e}^{-E/(k_BT)}\,\mathrm{d}E \quad (4)$$

The Maxwellian average opacity factors $\langle\pi/k^2 P^K_{jj'}\rangle_T$ can additionally be used to calculate the rotational de-excitation rate coefficients which correspond to a sum of the $\langle\pi/k^2 P^K_{jj'}\rangle_T$ over all values of K respecting the triangulation rules $|j'-j| \leqslant K \leqslant j'+j$, as well as to obtain the de-excitation rate coefficients among magnetic sublevels of the hyperfine energy structure:

$$R_{jF_1FM_F\to j'F_1'F'M_{F'}}(T) = \sum_K \begin{pmatrix} F' & F & K \\ -M_{F'} & M_F & M_{F'}-M_F \end{pmatrix}^2 \times \left\langle \frac{\pi}{k^2} P^K_{jF_1F,j'F_1'F'} \right\rangle_T \quad (5)$$

Table 1. Energy levels (in MHz) of the hyperfine structure of N_2H^+ for rotational levels j up to 7.

j	F_1	F	E(MHz)	j	F_1	F	E(MHz)	j	F_1	F	E(MHz)
0	1	2	0.0000	3	4	4	559030.0476	5	4	5	1397528.1846
0	1	1	0.0000	3	4	5	559030.4957	5	4	3	1397528.1979
0	1	0	0.0000	3	4	3	559030.5533	6	6	6	1956491.9348
1	1	0	93171.6167	3	2	2	559030.6708	6	6	5	1956492.4006
1	1	2	93171.9134	3	2	3	559031.0470	6	6	7	1956492.4368
1	1	1	93172.0484	3	2	1	559031.1749	6	7	7	1956494.0034
1	2	2	93173.4755	4	4	4	931700.6052	6	5	5	1956494.1900
1	2	3	93173.7723	4	4	5	931701.0433	6	7	6	1956494.4822
1	2	1	93173.9626	4	4	3	931701.0673	6	7	8	1956494.5253
1	0	1	93176.2608	4	5	5	931702.5885	6	5	4	1956494.6758
2	2	2	279516.4477	4	3	3	931702.9983	6	5	6	1956494.6989
2	2	3	279516.7030	4	5	6	931703.0686	7	7	7	2608587.5742
2	2	1	279516.7694	4	5	4	931703.0866	7	7	6	2608588.0344
2	3	3	279518.2351	4	3	4	931703.4423	7	7	8	2608588.0970
2	3	4	279518.6326	4	3	2	931703.5023	7	8	8	2608589.6732
2	3	2	279518.7426	5	5	5	1397525.3911	7	6	6	2608589.7877
2	1	1	279519.3252	5	5	4	1397525.8591	7	8	7	2608590.1420
2	1	2	279519.5369	5	5	6	1397525.8665	7	8	9	2608590.2109
2	1	0	279519.7891	5	6	6	1397527.4227	7	6	5	2608590.2628
3	3	3	559028.1346	5	4	4	1397527.7020	7	6	7	2608590.3168
3	3	4	559028.5123	5	6	5	1397527.9114				
3	3	2	559028.5682	5	6	7	1397527.9260				

Table 2. Coefficients $a^{(n)}_{j\rightarrow j'}$ ($n = 0$ to 5) of the polynomial fit (equation 6) to the rotational de-excitation rate coefficients. The excitation rate coefficients can be obtained by detailed balance.

j	j'	$a^n_{j\rightarrow j'}$					
		$n=0$	$n=1$	$n=2$	$n=3$	$n=4$	$n=5$
1	0	−9.931706	3.584804	−15.245108	33.839460	v−39.761834	16.655935
2	0	−9.811589	−5.691305	44.991466	−124.652942	139.711954	− 62.506917
3	0	−9.703441	−6.115553	43.305612	−124.023772	132.667058	− 60.521182
4	0	−10.060580	−0.384860	9.452541	−45.250728	29.831037	− 13.053514
5	0	−9.914293	0.738966	2.475379	−38.456589	7.891508	− 0.783440
6	0	−11.235536	12.801354	−40.272715	25.981939	−58.097044	21.013021
2	1	−9.284383	−5.957078	31.853595	−76.694685	78.369354	− 32.850466
3	1	−9.710740	−5.659005	39.895739	−111.195971	114.754040	− 49.378675
4	1	−9.528845	−5.485833	32.115275	−94.487472	85.008060	− 36.055763
5	1	−10.435428	4.378629	−6.786280	−27.477417	9.199626	− 5.914749
6	1	−10.100113	−0.087679	15.952518	−93.914494	72.194758	− 34.155143
3	2	−8.641272	−12.121146	52.195977	−110.173405	101.011094	− 38.475871
4	2	−10.293658	3.347989	−4.485154	−14.710317	6.387723	− 3.593830
5	2	−10.005844	−1.692313	24.355069	−99.644211	98.894073	− 47.195501
6	2	−10.268921	1.962685	3.468399	−58.655788	35.118357	− 17.186366
4	3	−9.140001	−7.641835	39.265680	−98.746972	100.371910	− 43.118890
5	3	−10.113276	1.028055	5.001249	−41.453097	34.745597	− 17.402125
6	3	−10.530111	5.456132	−14.229747	−13.638065	−4.539801	− 2.022254
5	4	−9.567617	−1.037751	0.211778	−2.149343	−15.493934	9.328017
6	4	−10.536518	6.101161	−20.004927	10.915303	−25.851330	8.086110
6	5	−9.341221	−3.281233	5.684067	−7.346877	−20.243780	14.433165

The Maxwellian average opacity factors are obtained using an analytical integration, and the opacity factors are interpolated by straight lines between calculated values. The latter calculations are carried out over essentially the entire energy range spanned by the Boltzmann distributions, i.e. up to 400 cm^{-1} in total energy. The number of energy points is carefully monitored to correctly reproduce all resonances in the opacity factors.

The rotational and hyperfine excitation rate coefficients can be obtained from the usual detailed balance equation with rotational energy levels calculated from $E_j = Bj(j + 1)$, where $B = 1.55397\ cm^{-1} \equiv 46586.85$ MHz is the rotational constant used in Daniel et al. (2004) and with hyperfine energy levels given in Table 1. It should be noted that hyperfine de-excitation rate coefficients are completely independent of the hyperfine energy values.

For rapid evaluation, the rotational de-excitation rate coefficients have been fitted by the analytical form used by Balakrishnan, Forrey & Dalgarno (1999), Dubernet & Grosjean (2002) and Grosjean, Dubernet & Ceccarelli (2003):

$$\log_{10} R(j \rightarrow j')(T) = \sum_{n=0}^{N} a^{(n)}_{j\rightarrow j'}\ x^n \qquad (6)$$

where $x = 1/T^{1/3}$ and where the coefficients $a^{(n)}_{j\rightarrow j'}$ are provided in Table 2.

Rather than fitting the hyperfine de-excitation rate coefficients, it is faster to fit the Maxwellian average opacity factors and to reconstruct the hyperfine de-excitation rate coefficients with equations (3) and (2). The Maxwellian average opacity factors are fitted with the same analytical form:

$$\log_{10} \left\langle \frac{\pi}{k^2} P^K_{jj'} \right\rangle_T = \sum_{n=0}^{N} a^{(K,n)}_{j'\rightarrow j}\ x^n \qquad (7)$$

The coefficients $a^{(K,n)}_{j\rightarrow j'}$ are given in Tables 3, 4 and 5 for all transitions among the seven lowest rotational levels. A fifth-order polynomial is required to cover the entire range of temperature and to provide a fitting error better than 0.1 per cent both on rate coefficients and on average opacity factors. Other analytical functions have been tried and were not able to reproduce the data as accurately as the chosen analytical function on the whole range of temperature. These fits are only valid in the temperature range from 5 to 50 K and they should not be used for extrapolation.

3 DISCUSSION

3.1 Rotational rate coefficients: comparison with Green's results

Up until now the only available rate coefficients for N_2H^+ excited by He were pure rotational excitation rate coefficients calculated by Green (1975), using a gas-electron model for the potential energy surface (PES). In previous work (Daniel et al. 2004) the influence of using a state-of-the art potential energy surface to calculate rotational excitation cross-sections was assessed by comparing with earlier results from Green (1975). The recent PES is well-suited for scattering calculations because it is extended to short enough He–N_2H^+ distances. Its reliability has been assessed by comparing energies of bound states and rotational constants with experimental data (Meuwly et al. 1996). Tables 6 and 7 give our calculated rotational de-excitation rates along with the percentage difference from Green's values (Green 1975). The percentage differences are larger for transitions with large Δj and varies in the range from a few per cent to 100 per cent. Overall the new rates are larger for all transitions and the differences decrease with increasing temperature. For the low Δj transitions, the differences are mainly due to different resonance features. It is known that the potential energy surface based on the gas-electron model is not of quantitative accuracy around the potential well. The differences for high Δj transitions are mainly sensitive to the choice of a larger basis set of rotational channels (including closed channels) in our computation.

Table 3. Coefficients $a_{j\rightarrow j'}^{(K,n)}$ ($n = 0$ to 6) of the polynomial fit (equation 7) to the Maxwellian average opacity factors $\langle \pi/k^2 P_{jj'}^K \rangle_T$ of equation (4). This table provides coefficients for transitions with j' up to 2.

$j' \rightarrow j$	K	$a_{j\rightarrow j'}^{n}$						
		$n=0$	$n=1$	$n=2$	$n=3$	$n=4$	$n=5$	$n=6$
0→ 0	0	0.224652	−11.769989	20.633469	−70.946168	130.897913	−126.442227	48.294301
1→ 0	1	0.317528	−14.817216	34.468780	−117.895704	223.002144	−223.028340	89.615035
2→ 0	2	0.641588	−19.672911	56.582898	−161.796896	256.159507	−229.090602	84.276222
3→ 0	3	0.685694	−20.234173	60.329621	−177.139515	281.579488	−259.800748	95.549266
4→ 0	4	0.315885	−14.914960	30.261682	−92.271336	141.991810	−151.413746	59.048280
5→ 0	5	−0.404248	−3.699048	−38.522972	132.891198	−278.692177	240.603933	−93.411997
6→ 0	6	−0.184607	−8.398788	−5.113934	19.190429	−83.492258	47.924680	−21.165793
	0	−0.038028	−7.062341	−6.773341	19.931368	−34.863568	27.207158	−8.876037
1→ 1	1	−0.119958	−10.806060	12.711101	−45.354382	78.920715	−75.193412	29.129175
	2	0.143585	−13.415930	28.501958	−96.899688	183.113583	−184.686769	74.510412
	1	−0.627344	1.659720	−74.658573	249.777190	−456.507432	419.428387	−158.054778
2→ 1	2	−0.141482	−10.752620	16.350426	−72.559600	153.466935	−173.200292	74.159681
	3	0.548207	−19.064565	58.497662	−180.496857	302.421503	−278.299604	103.824031
	2	0.012695	−9.634609	−2.999673	14.907227	−33.290774	5.069297	6.066027
3→ 1	3	0.018904	−12.242223	17.897211	−54.285460	77.164114	−79.429947	30.442760
	4	0.882992	−22.423706	68.546831	−185.176675	264.560880	−218.657440	71.968269
	3	0.919001	−22.181387	65.748444	−179.667170	253.278418	−220.144493	74.411481
4→ 1	4	0.104594	−13.723271	27.933690	−90.233523	136.912539	−140.191992	51.244624
	5	−0.534719	−1.470136	−50.913150	163.819194	−303.280610	252.024892	−90.591332
	4	−0.430158	−1.947988	−56.366928	206.399909	−432.069736	400.257128	−159.440413
5→ 1	5	−0.011153	−11.612973	13.107418	−34.629007	10.196988	−15.334133	−1.547148
	6	−0.219132	−7.857610	−6.128826	15.651229	−51.048931	15.275948	−4.036348
	5	−0.202140	−6.492579	−21.724189	84.844327	−216.916271	181.482168	−73.543919
6→ 1	6	0.081935	−13.470045	27.616337	−91.249366	112.854530	−130.409980	44.058768
	7	0.579619	−18.567728	48.604497	−131.256114	156.959857	−159.348317	53.648888
	0	−0.015458	−7.289588	−3.505112	8.948613	−21.141512	14.227386	−5.339242
	1	0.204187	−16.529186	59.812823	−241.371480	494.845639	−521.402093	216.194868
2→ 2	2	0.392767	−15.763637	32.554267	−79.545298	92.751924	−55.718608	8.870803
	3	−0.196907	−8.645444	−4.680708	25.267741	−69.138556	71.813460	−30.828878
	4	0.750100	−22.069520	75.668372	−225.563151	362.814946	−315.914956	110.840849
	1	−1.601704	16.156686	−157.598622	489.154505	−837.476810	727.154184	−262.468543
	2	0.269296	−16.587115	50.721086	−179.299116	325.776623	−327.432453	129.059292
3→ 2	3	0.663933	−19.815956	56.666101	−161.537140	245.874196	−219.993251	78.702984
	4	0.163877	−14.236849	28.911554	−82.133746	111.379765	−93.991171	28.790659
	5	−0.619306	0.621071	−67.318709	223.606258	−406.410223	358.273794	−132.168280
	2	−0.008224	−8.490692	−12.257808	49.709914	−119.372019	97.430493	−36.858104
	3	−0.135999	−9.153425	−1.577198	2.591092	−22.076777	2.166082	−1.466078
4→ 2	4	0.417724	−15.725771	29.833850	−68.573181	57.117349	−35.817399	2.710510
	5	0.036589	−12.043772	16.838365	−52.428612	67.121436	−74.084451	25.791576
	6	−0.412643	−4.817803	−24.126276	72.249767	−137.664295	99.125459	−33.393601
	3	0.285644	−12.149210	3.440859	22.470664	−122.692628	128.315848	−61.129188
	4	0.089440	−12.016651	12.382352	−28.118396	−5.904017	3.474520	−9.838076
5→ 2	5	0.120362	−12.005237	13.664620	−32.206639	2.512658	−6.057165	−5.527252
	6	−0.073138	−10.429199	7.252928	−19.376440	−5.637457	−13.553491	2.588218
	7	0.723866	−21.624321	72.462009	−218.177508	338.170505	−329.262732	122.502447
	4	0.142703	−10.608046	−1.432229	26.073558	−118.648107	94.286172	−41.739736
	5	0.000828	−11.691131	17.525660	−65.350650	84.040080	−121.503675	47.579579
6→ 2	6	−0.034823	−11.386331	16.930639	−63.131294	77.139375	−109.723172	40.677520
	7	−0.108592	−9.808575	1.887332	1.254130	−61.184357	31.096121	−14.715504
	8	−0.264640	−4.659464	−41.621809	162.726624	−366.626342	324.797002	−128.856580

Table 4. Coefficients $a^{(K,n)}_{j\rightarrow j'}$ ($n = 0$ to 6) of the polynomial fit (equation (7)) to the Maxwellian average opacity factors $\langle \pi/k^2 P^K_{jj'} \rangle_T$ of equation (4). This table provides coefficients for transitions with j' from 3 to 4.

	0	−0.087151	−6.088264	−9.643804	26.981575	−54.912255	35.570419	−11.584130
	1	−0.603084	−5.583048	5.513822	−116.388505	349.365901	−456.499015	212.511095
	2	0.333283	−13.453642	13.632239	−17.249547	−13.045354	18.649942	−10.334200
3→ 3	3	0.100156	−13.496707	30.700192	−115.740507	216.601885	−229.816423	93.525410
	4	0.688692	−21.333225	73.297977	−233.462046	398.624594	−378.744781	143.422899
	5	0.010386	−11.311673	11.390918	−31.470216	34.544760	−37.211482	12.791459
	6	−0.370001	−6.110609	−10.990071	15.148969	−7.830331	−28.845994	19.190886
	1	−0.310600	−5.258339	−12.402284	−13.795524	85.295648	−155.174792	75.891451
	2	−0.176815	−9.194438	5.128459	−40.579935	85.908095	−121.551560	52.855537
	3	0.868394	−23.213608	81.155830	−250.759698	407.118143	−383.235995	142.717153
4→ 3	4	0.248090	−14.775426	31.220503	−91.372804	120.783930	−112.669424	38.051804
	5	−0.259699	−5.730353	−27.271089	100.561557	−214.522861	191.319889	−75.124128
	6	−0.098593	−9.984892	5.911570	−16.649026	3.135972	−15.899933	4.777226
	7	0.561348	−19.660510	62.965269	−190.786178	298.044071	−278.102399	100.723719
	2	0.247550	−12.436478	14.704238	−46.149676	51.431643	−71.470704	24.933313
	3	0.145239	−13.776378	32.023756	−125.841697	231.370712	−272.177782	113.203866
	4	0.164895	−11.834601	7.112760	1.486308	−74.257843	75.471132	−38.585350
5→ 3	5	0.464812	−19.392625	70.281820	−247.866778	432.877221	−439.772591	168.563560
	6	−0.043952	−10.821678	11.224992	−37.909143	35.600250	−56.100407	19.840822
	7	−0.160588	−8.714283	−5.552758	28.016490	−95.709343	70.094191	−27.438844
	8	0.049912	−8.057251	−27.623674	129.011454	−307.276752	289.858039	−119.062637
	3	0.209139	−10.713853	−3.516652	32.625253	−125.605710	99.244663	−44.571551
	4	0.032458	−11.797069	18.431990	−75.577811	118.269741	−165.527932	67.547510
	5	0.059063	−12.030779	19.978004	−71.320132	91.630635	−125.815215	48.497426
6→ 3	6	−0.286365	−7.875011	−2.320053	−11.586336	5.622000	−65.322869	32.757659
	7	0.670727	−20.702653	64.813081	−188.746128	246.893824	−221.224678	67.447357
	8	−0.097729	−9.546685	−2.245470	17.609292	−93.719829	63.754627	−27.450202
	9	−0.505848	−3.713049	−34.734745	105.901607	−219.891595	157.472282	−56.221403
	0	−0.005854	−7.284202	−1.203138	−0.635349	−14.640032	−7.793579	4.475816
	1	−3.936578	49.536188	−358.249133	1111.311770	-1903.162116	1663.552939	−600.705095
	2	0.237601	−16.353759	62.293725	−271.123217	579.685704	−658.982498	286.823506
	3	0.564148	−18.611138	51.181314	−149.661204	215.211734	−190.972778	63.462833
4→ 4	4	0.256162	−15.267464	42.789215	−163.668242	315.193189	−350.980600	148.314838
	5	0.301331	−16.666618	53.284749	−194.699530	353.807164	−364.546126	143.426363
	6	−0.144679	−8.809647	−3.998415	21.840605	−80.715784	74.923023	−33.675155
	7	0.082388	−12.733608	21.811753	−65.148168	79.512684	−78.748802	25.785652
	8	0.610474	−16.194172	18.803344	−5.450635	−90.802428	121.453960	−60.637595
	1	−1.173814	4.097730	−41.710821	−23.504657	286.409932	−524.195664	276.988985
	2	−0.165727	−7.386313	−14.947999	45.170183	−107.291560	74.223188	−29.971518
	3	−0.013106	−8.541183	−14.835728	69.200628	−181.453187	159.419522	−64.217781
	4	0.053023	−12.231169	21.764864	−82.593254	130.912203	−157.330237	62.456776
5→ 4	5	−0.267691	−6.738102	−14.580774	43.528044	−102.301751	65.471503	−24.171627
	6	−0.295940	−7.220985	−8.488860	14.874575	−40.269181	−2.175752	5.339309
	7	0.499458	−18.328802	51.289978	−144.883119	180.400502	−151.748162	43.672317
	8	0.190598	−13.714334	22.500510	−62.239966	59.070261	−64.064385	19.138389
	9	−0.624224	−2.132526	−42.665521	123.891024	−228.978328	169.826270	−59.495243
	2	−0.366458	−3.333574	−38.164976	110.380698	−206.703003	125.196892	−37.261198
	3	−0.607648	−0.561627	−58.611630	192.230451	−388.717753	331.963207	−130.630777
	4	0.265992	−14.123106	26.985326	−79.191421	84.569232	−104.085651	35.704623
	5	−0.359760	−5.642319	−20.280287	58.396528	−134.330386	74.931443	−23.202565
6→ 4	6	−0.005344	−11.462373	16.353604	−61.488780	75.974960	−112.039211	43.539990
	7	0.935947	−26.649654	112.328060	−374.786340	627.658714	−614.175525	229.009740
	8	0.461501	−18.818041	61.003486	−199.335822	296.648722	−290.880983	101.444128
	9	0.019863	−11.862812	13.828973	−47.366038	43.261747	−77.812739	29.752385
	10	1.036214	−27.433607	104.789678	−322.510426	506.698484	−488.893048	179.991988

Table 5. Coefficients $a_{j\rightarrow j'}^{(K,n)}$ ($n = 0$ to 6) of the polynomial fit (equation 7) to the Maxwellian average opacity factors $\langle \pi/k^2 P_{jj'}^K \rangle_T$ of equation (4). This table provides coefficients for transitions with j' from 5 to 6.

	0	−0.012974	−7.110006	−1.675775	1.274181	−29.247058	−0.541101	0.348546
	1	−2.034684	23.464533	−213.168333	697.090022	-1285.285288	1186.584314	−459.411996
	2	−0.808357	1.969390	−64.462476	178.244162	−295.243157	204.444377	−62.904648
	3	0.579834	−19.072525	58.936133	−195.531094	328.480264	−343.729115	135.732008
	4	−0.160358	−7.658390	−13.111357	51.100128	−138.657407	118.976591	−51.105172
5→ 5	5	−0.452099	−3.995443	−31.068552	93.679259	−185.270247	129.990942	−42.112548
	6	0.064893	−12.776220	26.916781	−102.445638	168.268572	−195.839786	79.627020
	7	0.922436	−26.798664	116.890078	−402.079616	702.637534	−681.257397	256.454066
	8	0.778920	−24.259008	99.759443	−344.285380	597.714894	−584.137215	219.948596
	9	0.197010	−15.129442	37.506312	−133.086762	218.043397	−238.106499	93.489062
	10	0.515174	−20.967250	74.696769	−252.997722	432.994790	−440.706474	171.644144
	1	−3.966852	47.970394	−320.329078	893.366911	-1378.437101	1027.426350	−316.916255
	2	0.132854	−12.494550	23.357566	−101.368725	175.587687	−223.987599	90.749450
	3	0.570507	−17.193067	36.824356	−84.754585	53.703036	−43.456120	2.730828
	4	−0.684911	0.151313	−59.327805	188.347540	−365.506190	288.359023	−103.511068
	5	0.064755	−12.125355	20.295048	−68.840325	79.675122	−106.472559	37.962265
6→ 5	6	−0.632486	−1.234003	−50.536314	161.703600	−326.570804	261.657951	−97.248507
	7	−0.203610	−7.953536	−5.040759	−3.668997	−6.044545	−53.088019	26.134637
	8	0.881886	−27.940379	134.198294	−497.509680	934.687172	−972.967477	389.744966
	9	0.395703	−19.311775	71.891971	−268.530561	481.760350	−514.263216	203.155542
	10	0.351195	−17.306100	45.440462	−144.971251	205.890140	−216.040859	76.731516
	11	1.736617	−31.231176	94.214683	−220.038623	229.436047	−156.345177	28.143003
	0	−0.097197	−5.662817	−10.579469	30.497165	−92.540382	45.935740	−16.653483
	1	−3.286006	39.362975	−287.546973	857.017502	-1457.892424	1243.562140	−453.192903
	2	0.562380	−18.175065	55.299407	−185.529095	296.218406	−316.227930	120.270611
	3	0.377540	−14.392809	20.251752	−36.666775	−25.067002	27.222751	−24.278065
	4	−0.613532	−1.375437	−46.371682	141.900131	−279.376774	208.203580	−73.773412
	5	−0.009806	−10.305333	4.954184	−7.786333	−47.518668	23.799265	−15.277959
6→ 6	6	−0.179020	−7.727442	−10.679998	30.551092	−92.511917	46.645178	−17.835288
	7	−1.494802	12.243631	−135.648924	427.500455	−780.574886	668.448649	−247.813033
	8	−1.810009	16.725559	−159.840209	494.275196	−881.169618	745.213665	−270.668470
	9	−1.198463	4.481203	−72.236837	178.387775	−272.534861	141.904560	−28.342274
	10	0.583481	−21.475097	79.039536	−284.633579	501.863447	−529.566038	208.533669
	11	−0.005931	−12.428011	18.256313	−81.118929	135.682699	−189.939754	79.825520
	12	−0.444481	−4.710422	−36.483954	118.353163	−258.769728	209.480849	−83.131091

Table 6. Our calculated rotational rates at T = 10 K (in units of 10^{-12} cm^3 s^{-1}). Values in bracket give the percentage difference from Green's values (Green 1975). The first column gives the initial levels.

	0		1		2		3		4		5		6	
0	0.00	(0.00)	221.33	(22.46)	81.82	(21.78)	17.36	(23.13)	2.38	(21.80)	0.29	(124.77)	0.02	(142.15)
1	115.44	(22.11)	0.00	(0.00)	118.48	(−1.55)	25.17	(23.94)	3.67	(51.45)	0.49	(73.60)	0.03	(65.47)
2	62.63	(21.75)	173.96	(−1.30)	0.00	(0.00)	66.08	(16.43)	11.02	(24.35)	1.16	(73.31)	0.06	(1.25)
3	36.30	(23.21)	100.96	(23.90)	180.59	(16.44)	0.00	(0.00)	42.44	(16.55)	3.42	(43.67)	0.21	(22.51)
4	23.10	(21.20)	68.38	(51.52)	140.08	(25.35)	197.49	(17.02)	0.00	(0.00)	18.33	(23.52)	1.13	(10.34)
5	21.71	(117.97)	69.29	(74.93)	112.80	(71.85)	121.59	(42.90)	140.18	(23.16)	0.00	(0.00)	9.93	(5.30)
6	22.23	(109.89)	58.28	(62.65)	72.90	(5.82)	91.50	(23.13)	106.30	(9.44)	122.60	(4.88)	0.00	(0.00)

Table 7. Our calculated rotational rates at T = 40 K (in units of 10^{-12} cm^3 s^{-1}). Values in bracket give the relative difference with Green's values (Green 1975). The first column gives the initial levels.

	0		1		2		3		4		5		6	
0	0.00	(0.00)	253.47	(15.71)	138.74	(1.20)	89.26	(−1.10)	49.42	(−12.64)	40.56	(61.27)	21.58	(104.01)
1	94.49	(15.07)	0.00	(0.00)	191.63	(−1.85)	99.75	(8.30)	62.38	(8.64)	42.89	(35.22)	22.13	(59.00)
2	38.81	(1.19)	143.78	(−1.65)	0.00	(0.00)	151.01	(−1.49)	93.99	(25.24)	51.58	(30.17)	22.65	(14.58)
3	24.93	(−1.25)	74.75	(8.37)	150.82	(−1.47)	0.00	(0.00)	143.06	(8.16)	62.43	(29.87)	29.52	(23.58)
4	16.78	(−12.80)	56.82	(8.70)	114.11	(25.65)	173.92	(8.42)	0.00	(0.00)	100.00	(5.91)	43.47	(19.01)
5	19.65	(61.17)	55.74	(34.96)	89.37	(30.10)	108.32	(29.77)	142.79	(5.95)	0.00	(0.00)	76.66	(6.77)
6	17.32	(105.70)	47.65	(60.11)	65.00	(15.27)	84.83	(24.64)	102.73	(19.90)	126.67	(6.69)	0.00	(0.00)

3.2 Hyperfine rate coefficients: comparison with other methods

In the simplest approach used in astrophysical applications (Guilloteau & Baudry 1981), it is assumed that the hyperfine de-excitation rate coefficients are proportional to the degeneracy $(2F' + 1)$ of the final hyperfine level and independent of the initial hyperfine level. This simple method corresponds to a statistical reorientation of the rotational quantum number j after collision (Alexander & Dagdigian 1985) and is not suitable at low temperature as is shown in Fig. 1. Indeed, Fig. 1 shows that for a given j, F_1, F to j', F'_1 transition, the relative behavior of hyperfine rate coefficients among final F' state changes with temperature and the highest rate coefficient is not always the one with the highest final F' state.

If the average opacity factors $\langle \pi/k^2 P^K_{jj'} \rangle_T$ decrease for increasing K, the hyperfine rate coefficients should obey propensity rules given by the behaviour of Wigner-6j coefficients (Daniel et al. 2004), combined with both the range of allowed values for the quantum number F' and the degeneracy factor $(2F' + 1)$. At low temperatures the decrease of the average opacity tensors is not observed and their relative magnitude varies with temperature (see Fig. 2). This explains why the relative ratios of hyperfine rate coefficients associated with a rotational transition $j \rightarrow j'$ vary with temperature (see Fig. 1). Calculations are therefore required to obtain the relative intensities of the two-spin hyperfine rate coefficients. Table 8 gives an example at $T = 20$ K of exceptions to the propensity rules due to Wigner-6j coefficients for the transition $j = 4 \rightarrow j' = 3$.

The second method widely used is the one employed by Neufeld & Green (1994) in the case of HCl–He. They used the Infinite Order Sudden (IOS) formula derived by Corey & McCourt (1983) for one spin [which is similar to the expression found by Varshalovich & Khersonskii (1977)]. Similarly, we derive the formula for the case of two nuclear spins by replacing our CC scattering matrices by IOS matrices in equation (13) of Daniel et al. (2004) and the IOS rate coefficients among hyperfine levels are :

$$R^{\rm IOS}(jF_1F \rightarrow j'F'_1F')(T) = [jj'F_1F'_1F'] \times \sum_K \left\{ \begin{array}{ccc} j & j' & K \\ F'_1 & F_1 & I_1 \end{array} \right\}^2 \times \left\{ \begin{array}{ccc} F_1 & F'_1 & K \\ F' & F & I_2 \end{array} \right\}^2 \times \left(\begin{array}{ccc} j & j' & K \\ 0 & 0 & 0 \end{array} \right)^2 R_K(T), \quad (8)$$

with the fundamental rates $R_K(T)$ given by :

$$R_K(T) = R^{\rm IOS}(0 \rightarrow K) = [K] R^{\rm IOS}(K \rightarrow 0) \quad (9)$$

These formulae apply the IOS approximation to both the rotational and the hyperfine structure. The following observations might cast doubt about the validity of this approach in the case of N_2H^+: (i) it is known that the IOS approximation breaks down when internal energy spacings are large compared with the collision energy, which is certainly the case for the rotational structure at the collision energies of interest here; and (ii) the He–N_2H^+ has a very deep potential well compared to the collision energy and the IOS approximation has been proved to be invalid (Goldflam, Kouri & Green 1977) in such a case because of strong couplings to closed channels (Feshbach resonances). Therefore we implemented an improved method proposed by Neufeld & Green (1994), in which the IOS 'fundamental' rates $R^{\rm IOS}(0 \rightarrow K)$ are replaced by CC 'fundamental rates' $R^{\rm CC}(0 \rightarrow K)$ in equation (8) and where a scaling relationship is used. We also tested the two common ways (Green 1985) often used to obtain de-excitation rate coefficients: either de-dexcitation rate coefficients are obtained using de-excitation fundamental rates $[K]R^{\rm CC}(K \rightarrow 0)$, or excitation rate coefficients are obtained using excitation fundamental rates $R^{\rm CC}(0 \rightarrow K)$ and de-excitation rates are obtained using the detailed balance relationship. In both cases we found that the IOS approximations tend to increase the flux in the

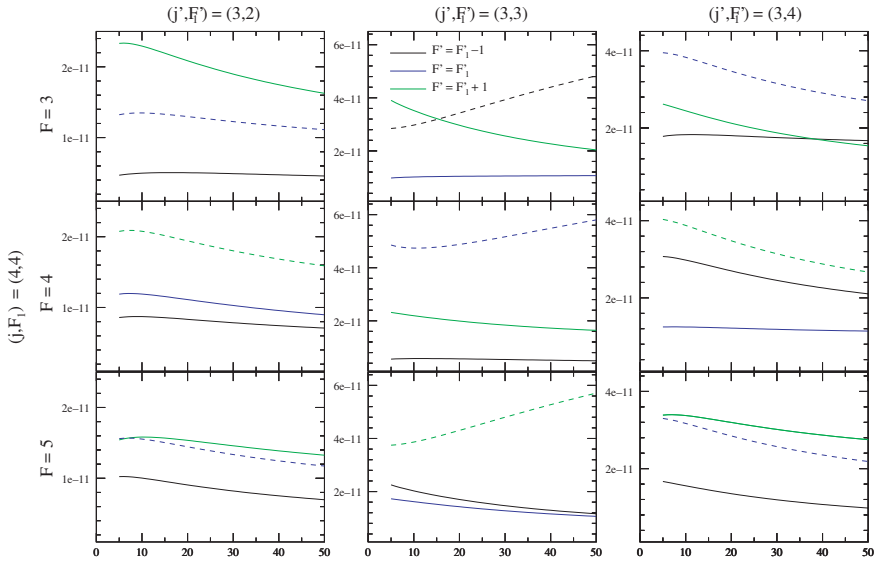

Figure 1. Hyperfine rate coefficients (in $cm^3\ s^{-1}$) as a function of temperature (in K), given by equation (2) from the states $(j,\ F_1) = (4, 4)$ and $F = 3, 4, 5$ to the states associated with $j' = 3$, i.e. $F'_1 = 2, 3, 4$ and $F' = F'_1 - 1$ (black), F'_1 (blue), $F'_1 + 1$ (green). Each sub-figure corresponds to fixed values of j, F_1, F, j', F'_1. The rate coefficients in dashed lines are the rates expected to be of highest magnitude according to regular propensity rules from the behaviour of Wigner-6j coefficients.

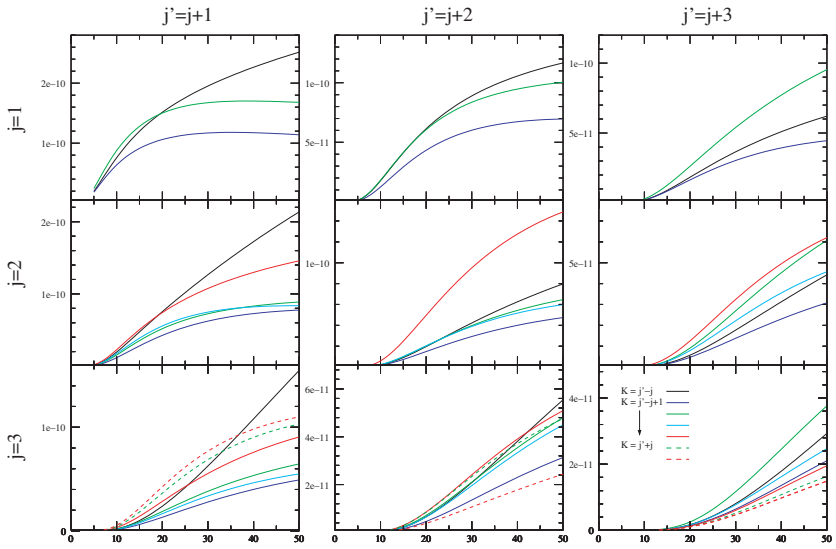

Figure 2. Averaged opacity tensors $\langle \pi/k^2 P^K_{j'j} \rangle_T$ as a function of temperature (in K). They do not decrease with K and their relative magnitude vary with temperature.

Table 8. Hyperfine rate coefficients for the $j = 4 \rightarrow j' = 3$ transition at $T = 20$ K. For given initial F_1, F, and final F'_1, a bold number indicates the largest rate coefficients among the final F', an italic number indicates the expected largest rate coefficients according to propensity rules due to Wigner-6j coefficients behaviours.

		2			3			4		
		1	2	3	2	3	4	3	4	5
3	2	**27.69**	17.56	8.78	8.78	*19.21*	**27.74**	2.74	16.65	**57.95**
3	3	8.39	**28.95**	16.69	13.72	15.98	**26.03**	12.31	29.65	**35.39**
3	4	3.31	9.75	**40.98**	15.41	**20.25**	20.08	**35.69**	27.85	13.80
4	3	5.04	*12.97*	**20.86**	**34.25**	10.42	29.65	18.00	**34.70**	21.23
4	4	8.33	11.12	**19.42**	5.65	**48.77**	19.89	26.99	12.16	**34.78**
4	5	9.06	*14.45*	**15.35**	17.01	14.27	**43.03**	13.51	*28.46*	**31.96**
5	4	1.35	8.50	**33.32**	13.05	**26.59**	17.18	**57.65**	23.85	5.62
5	5	6.04	15.71	**21.42**	19.65	9.36	**27.81**	16.92	**48.89**	21.31
5	6	*15.87*	**17.35**	9.94	8.68	*21.75*	**26.39**	3.11	15.84	**68.18**

$\Delta F = \Delta F_1 = \Delta j$ transitions by a factor of 2 and, that this feature is even stronger when using excitation fundamental rates. It should be noted that the use of the IOS expression of equation (8) associated to the fundamental rates $R^{CC}(0 \rightarrow K)$ is equivalent to approximate the $\langle \pi/k^2 P^K_{jj'} \rangle_T$ given in equation (4) by:

$$\left\langle \frac{\pi}{k^2} P^K_{jj'}(\mathrm{IOS}) \right\rangle_T = [jj'] \begin{pmatrix} j & j' & K \\ 0 & 0 & 0 \end{pmatrix}^2 R^{CC}(0 \rightarrow K). \qquad (10)$$

These tensors rapidly decrease with K and vanish except if K has the same parity as $j + j'$, which implies that in the sudden limit the propensity rules are only given by angular algebra. It has been shown above that due to the presence of resonances, the calculated CC $\langle \pi/k^2 P^K_{jj'} \rangle_T$ do not have this straightforward behaviour.

4 SUMMARY

Helium de-excitation rate coefficients have been determined among rotational and hyperfine levels of N_2H^+ using the recoupling technique of Daniel et al. (2004) with CC spin-free calculations. Two simple approaches often used to calculate the same quantities in the absence of hyperfine calculations were assessed. In particular, the scaled IOS approach (Neufeld & Green 1994) was found to provide no good estimate of hyperfine propensity rules due to the presence of Feshbach resonances which is related to the strong attraction in He–N_2H^+. We believe that the scaled IOS approach could become valid for N_2H^+ at higher temperature once the resonance region has a small contribution to the kinetic Boltzmann distribution. This conclusion can be generalized to the determination of fine or hyperfine rate coefficients for all collisional systems. Fits of both the de-excitation rotational rate coefficients and the average opacity factors are provided, they are only valid in the temperature range from 5 to 50 K. Fitting coefficients for transitions among rotational levels up to $j = 6$ and for hyperfine transitions both among elastic and inelastic rotational levels up to $j = 6$, the routine to reconstruct the various rotational and hyperfine rate coefficients can be obtained from the authors (M-LD) and will be made available on the website.[1]

ACKNOWLEDGMENTS

The authors thank P. Caselli and L. Dore for providing their latest results on the hyperfine structure of N_2H^+. Most scattering calculations were performed at the IDRIS-CNRS (Institut du developpement et des ressources en informatique scientifique du

[1] http://www.obspm.fr/basecol

Centre National de la Recherche Scientifique) and CINES under project 041472. MM acknowledges financial support from the Swiss National Science Foundation for a Förderungsprofessur.

REFERENCES

Alexander M. H., Dagdigian P. J., 1985, J. Chem. Phys., 83, 2191
Balakrishnan N., Forrey R. C., Dalgarno A., 1999, ApJ, 514, 520
Belloche A., André P., Despois D., Blinder S., 2002, A&A, 393, 927
Bergin E. A., Alves J., Huard T., Lada C. J., 2002, ApJ, 570, L101
Caselli P., Benson P. J., Myers P. C., Tafalla M., 2002, ApJ, 572, 238
Caselli P., Myers P. C., Thaddeus P., 1995, ApJ, 455, L77+
Cernicharo J., Guelin M., 1987, A&A, 176, 299
Corey G. C., McCourt F. R., 1983, J. Phys. Chem., 87, 2723
Daniel F., Dubernet M.-L., Meuwly M., 2004, J. Chem. Phys., 121, 4540
Dubernet M.-L., Grosjean A., 2002, A&A, 390, 793
Goldflam R., Kouri D. J., Green S., 1977, J. Chem. Phys., 67, 5661
Gonzalez-Alfonso E., Cernicharo J., 1993, A&A, 279, 506
Gordy W., Cook R. L., 1984, Techniques of Chemistry Vol 18, Microwave molecular spectra. Wiley Interscience, New York
Green S., 1975, ApJ, 201, 366
Green S., 1985, J. Phys. Chem., 89, 5289
Grosjean A., Dubernet M.-L., Ceccarelli C., 2003, A&A, 408, 1197
Guilloteau S., Baudry A., 1981, A&A, 97, 213
Hotzel S., Harju J., Walmsley C. M., 2004, A&A, 415, 1065
Meuwly M., Nizkorodov S. A., Maier J. P., Bieske E. J., 1996, J. Chem. Phys., 104, 3876
Neufeld D. A., Green S., 1994, ApJ, 432, 158
Tafalla M., Myers P. C., Caselli P., Walmsley C. M., 2004, A&A, 416, 191
Thaddeus P., Turner B. E., 1975, ApJ, 201, L25
Varshalovich D. A., Khersonskii V. K., 1977, ApJ, 18, 167

This paper has been typeset from a TEX/LATEX file prepared by the author.